Experimental study of the macroscopic quantum fluctuations of partially coherent stimulated Raman scattering

I. A. Walmsley and M. G. Raymer
The Institute of Optics, University of Rochester, Rochester, New York 14627
(Received 18 June 1985)

The large-scale fluctuations of Stokes light generated by stimulated Raman scattering have been studied experimentally by measuring the probability density function of Stokes pulse energies. The size and shape of the scattering region and the rate of collisional dephasing of the scatterers determine the degree of coherence of the Stokes light, and this in turn determines the form of the probability distribution. The experiments were performed for several diameters of the scattering volume, and for various collisional dephasing rates. The results of the experiments are compared to a recently reported quantum theory, and qualitative agreement is found. The need for a more accurate theory is pointed out.

I. INTRODUCTION

The behavior of individual light pulses generated by stimulated Raman scattering (SRS) provides one of few known examples of full-scale quantum fluctuations in the macroscopic domain. In particular, the energy of such pulses has been shown, both theoretically[1] and experimentally,[2–4] to undergo large fluctuations from pulse to pulse when the Raman gain remains unsaturated. The Raman system is macroscopic in that it is composed of about 10^{20} molecules and between 10^6 and 10^{16} Stokes photons. The actual number of Stokes photons generated in any given pulse is, however, highly unpredictable. This is a large-scale manifestation of the quantum noise associated with spontaneous scattering. In the case where there is a negligible amount of collisional dephasing, the situation arises that a macroscopic system, which starts out in a well-defined (pure) quantum state, then evolves in time according to Hamiltonian dynamics, and ends up in a pure state having highly unpredictable values of its macroscopic physical observables.

Examples of other macroscopic systems in which quantum fluctuations have been observed include transient laser buildup,[5] amplified spontaneous emission,[6] two-level superfluorescence,[7,8] and bistable two-mode laser operation.[9] Each of these involves the amplification by *stimulated emission* of microscopic quantum noise associated with the *spontaneous fluorescence* in a medium having a population inversion. SRS, in contrast, involves amplification by *stimulated scattering* of quantum noise associated with *spontaneous scattering*, in a medium which has no population inversion in the usual sense.

When an intense laser pulse of frequency ω_L is incident on a Raman active medium, light may be scattered at a red-shifted frequency ω_S, the Stokes frequency, leaving the medium in an excited state. Photons are scattered spontaneously at first, whilst at later times stimulated scattering can lead to the formation of a Stokes pulse with a macroscopic amount of energy. Since the source of the scattering is quantum noise, the final number of photons produced in a given pulse will be highly uncertain. The proper description of Stokes light generation requires a quantized field theory,[10,11] in contrast to the amplification of an externally applied Stokes field, which can be well described by a semiclassical theory.[12]

The quantum theory of Stokes generation has been used to derive the probability density function $P(W)$ for Stokes pulse energies W, for both unsaturated gain[1,3,13,14] and saturated gain.[15] It is predicted that the shape of the distribution is determined by the amount of temporal incoherence in the scattered light, which results from collisional dephasing,[3,14] and by the amount of spatial incoherence which results from the finite transverse extent of the emitting volume.[13]

In the case where there is little dephasing and the source is approximately one dimensional the distribution of Stokes pulse energies is close to a negative exponential. One may think of the SRS process as amplifying the zero-point radiation field, which is Gaussian distributed, leading to an exponential distribution for the intensity (and energy). As either temporal or spatial incoherence increase, the normalized standard deviation of the distribution decreases and the most probable value of the energy tends to the mean energy. These effects arise from the averaging together of statistically independent random fields. Measurement of the pulse-energy distributions can provide insight into the nature of the spontaneous initiation and amplification of light scattering, and is closely related to similar studies in two-level superfluorescence[7,8] and amplified spontaneous emission.[6]

We will distinguish several regimes in SRS. The "transient regime" is to be defined as that regime of SRS in which collision-induced temporal incoherence plays a negligible role in determining the properties of the generated Stokes light. If 2Γ is the rate of dephasing collisions in the medium and τ_L the length of the pump pulse, then $\Gamma\tau_L \to 0$ is clearly a sufficient criterion to guarantee the transient regime. The condition $\Gamma\tau_L < 1$ is sometimes used as a criterion for this regime, although this is overly restrictive. The necessary condition is that $\Gamma\tau_L < gL$ where g is the steady-state Raman gain coefficient, and L is the length of the interaction region.[16,17]

This is because the time required for the Stokes intensity to reach steady state depends on the gain. There has been some interest in the best choice of criterion for delimiting the transient regime. Since the probability distributions we have measured are sensitive to the amount of temporal coherence, and thus to the regime in which the scattering occurs, we believe that the experiments reported here will help clarify the issue.

The present paper gives a full account of experimental studies of the probability density function of Stokes pulse energies, and a comparison with a recently developed theory. This theory is a quantum-mechanical treatment which includes collisional dephasing and three-dimensional spatial propagation under unsaturated gain conditions. It is expounded in detail in a separate paper.[17]

The experiments were carried out by scattering pulses from a frequency-doubled Nd:YAG laser in hydrogen in the unsaturated gain regime. The pump laser pulse had a duration of 10 nsec. This meant that the pump pulse was between 8 and 40 times longer than the time between collisions, giving $\Gamma\tau_L \sim 16-80$. The Fresnel number of the interaction region was varied between $F=0.3$ and 4. The gain coefficient gL was in the range 8–12 and thus the experiments were in the steady-state regime or the regime intermediate between transient and steady state.

In explaining our experiments using the aforementioned quantized field theory it is useful to introduce the concept of "coherence modes," the excitation strengths of which determine the shape of the pulse-energy distribution $P(W)$. These modes are a complete set of electric field distributions whose forms are determined by the regime in which the scattering takes place and by the shape of the interaction volume, in other words by the degree of temporal and spatial coherence in the scattering process. A one-dimensional theory, including dephasing due to collisions, requires consideration of the temporal coherence modes alone,[3] whereas a full three-dimensional treatment must also include the spatial modes, since these describe the diffraction of the light generated in the scattering volume.[13,17]

Based on recent success in modeling experiments in two-level superfluorescence,[7,8] it was originally believed[1] that if the Fresnel number of the interaction region was close to unity then a theory using only one-dimensional propagation, and consequently ignoring diffraction, would be adequate for describing SRS statistics. We have found through theory and experiment that this is not the case. The fluctuation statistics of the pulse energies are significantly affected by the finite transverse spatial extent of the interaction volume, since higher-order spatial coherence modes are excited, even when $F \sim 1$.

In Sec. II the theory of Ref. 17 is briefly reviewed and important experimental parameters are introduced. In Sec. III the experiments and results are described. In Sec. IV a comparison is made between the theory and experiments, and in Sec. V the conclusions are given.

II. SUMMARY OF THEORY

In this section we give a brief overview of the theory of Stokes pulse-energy fluctuations, with a more complete treatment being given in a separate paper.[17] This theory treats simultaneously the effects of collisional dephasing[3,14] and three-dimensional spatial propagation,[13] each of which has been treated individually before. The objective of the theory is to calculate the probability distribution function $P(W)$ for the observed Stokes pulse energy W, when the gain remains unsaturated, and the Fresnel number of the interaction region is of the order of, or greater than, unity ($F \gtrsim 1$).

The medium is modeled as a molecular gas with average density N, and with energy levels as shown in Fig. 1. An intense laser beam of frequency ω_L, which is off resonance with the upper states of the molecule, is assumed to uniformly pump a cylindrically shaped volume of the medium with radius a and length L. The Fresnel number of this interaction volume is defined to be $F=\pi a^2/\lambda_S L$, where λ_S is the Stokes wavelength. The Fresnel number determines the degree of spatial coherence of the generated Stokes light. If $F \sim 1$ the diffraction angle $(\lambda_S/2a)$ of the Stokes light is approximately equal to the geometrical angle $(2a/L)$ of the gain volume, and so the Stokes light has a high degree of spatial coherence. If $F > 1$ then not as much spatial filtering of the Stokes light by the gain region occurs, and it remains spatially incoherent.

Few molecules are excited out of their ground states and the laser field amplitude $E_L(\mathbf{r},t)$ is not significantly changed during the interaction. The Maxwell-Bloch operator equations governing the behavior of the Stokes field operator $\hat{E}_S(\mathbf{r},t)$ and the molecular transition operator $\hat{Q}(\mathbf{r},t)$ in a medium with negligible group velocity dispersion are[10]

$$\left[\nabla^2-\frac{1}{c^2}\frac{\partial^2}{\partial t^2}\right]\hat{E}_S^{(+)}(\mathbf{r},t)e^{-i(\omega_S t-k_S z)} = \frac{2\kappa_2^*}{c\omega_S}\frac{\partial^2}{\partial t^2}E_L^*(\mathbf{r},t)\hat{Q}(\mathbf{r},t)e^{-i(\omega_S t-k_S z)}, \quad (1)$$

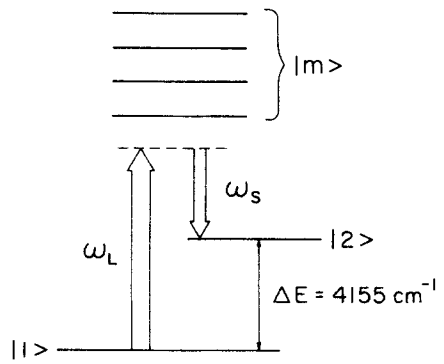

FIG. 1. Energy-level scheme for stimulated Raman scattering from the $Q(1)$ vibrational transition in hydrogen. The molecule is initially in its ground state $|1\rangle$ when an intense laser pulse, with frequency ω_L, excites it to a virtual level with large detuning from the manifold of states $|m\rangle$. Scattered photons, with frequency ω_S, are generated, leaving the molecule in the excited state $|2\rangle$.

$$\frac{\partial}{\partial t}\hat{Q}(\mathbf{r},t)=-\Gamma\hat{Q}(\mathbf{r},t)-i\kappa_1^*E_L(\mathbf{r},t)\hat{E}_S^{(+)}(\mathbf{r},t)+\hat{F}(\mathbf{r},t)\ , \tag{2}$$

where the coupling constant κ_1 is given by

$$\kappa_1=\frac{1}{\hbar^2}\sum_m d_{3m}d_{m1}\left[\frac{1}{\omega_{m1}-\omega_L}+\frac{1}{\omega_{m1}+\omega_S}\right]\ , \tag{3}$$

and the d_{ij} are dipole matrix elements. The constant κ_2 is related to κ_1 via $\kappa_2=2\pi\hbar\omega_S\kappa_1^*/c$. The well-known steady-state gain coefficient is related to these constants by

$$g=2\kappa_1\kappa_2|E_L|^2/\Gamma\ . \tag{4}$$

The linewidth Γ and delta-correlated random force $\hat{F}(\mathbf{r},t)$ model the effects of collision-induced phase fluctuations of $\hat{Q}(\mathbf{r},t)$, which describes the molecular vibration. As the gain increases, the Stokes light gets spectrally narrower, and therefore more temporally coherent. It turns out[17] that if $\Gamma\tau_L/gL\lesssim 1$ the Stokes light has a high degree of temporal coherence. The combination $\Gamma\tau_L/gL$ will be referred to as the "temporal coherence parameter."

It is possible to solve Eqs. (1) and (2) analytically, using techniques similar to those in Ref. (13), for the Stokes field operator $\hat{E}_S^{(+)}(\mathbf{r},t)$, in terms of the initial values of the molecular transition operator, $\hat{Q}(\mathbf{r},0)$, and the noise operator, $\hat{F}(\mathbf{r},t)$. The properties of these operators are determined by

$$\langle\hat{Q}^\dagger(\mathbf{r},0)\hat{Q}(\mathbf{r}',0)\rangle=\frac{1}{N}\delta^3(\mathbf{r}-\mathbf{r}')\ , \tag{5a}$$

$$\langle\hat{F}^\dagger(\mathbf{r},t)\hat{F}(\mathbf{r}',t')\rangle=\frac{2\Gamma}{N}\delta^3(\mathbf{r}-\mathbf{r}')\delta(t-t')\ . \tag{5b}$$

The solution may be represented as

$$\hat{E}_S^{(+)}(\mathbf{r},t)=\int K_1(\mathbf{r},\mathbf{r}',t)\hat{Q}(\mathbf{r}',0)d^3r' + \int\int K_2(\mathbf{r},\mathbf{r}',t,t')\hat{F}(\mathbf{r}',t')d^3r'dt'\ , \tag{6}$$

where K_1 and K_2 are propagation kernels involving the parameters Γ, g, and a.

We define the Stokes pulse-energy operator, in units of photons per pulse, to be

$$\hat{W}=\frac{c}{2\pi\hbar\omega_S}\int d^2\rho\int dt\,\hat{E}_S^{(-)}(\mathbf{r},t)\hat{E}_S^{(+)}(\mathbf{r},t)\ , \tag{7}$$

integrated over the output face of the cylinder ($z=L$). Then the probability density function for pulse energy is given by

$$P(W)=\frac{1}{2\pi}\int d\xi\exp(-i\xi W)\langle\exp(i\xi\hat{W})\rangle\ , \tag{8}$$

where the brackets indicate an expectation value taken with the system in its initial state.

The concept of coherence modes follows neatly from this formalism. We expand the field operator, given by Eq. (6), in terms of a set of modes

$$\hat{E}_S^{(-)}(\mathbf{r},t)=\sum_n\sum_k\beta_n^{1/2}\phi_n(\rho)\psi_k(t)\hat{b}_k^{(n)}\ , \tag{9}$$

where the $\hat{b}_k^{(n)}$ operators can be chosen to be uncorrelated

$$\langle\hat{b}_k^{(n)\dagger}\hat{b}_l^{(m)}\rangle=\lambda_k\delta_{kl}\delta_{nm} \tag{10}$$

and the $\phi_n(\rho)$ and $\psi_k(t)$ are assumed to form an orthonormal basis. The $\phi_n(\rho)$ are the "spatial coherence modes" and the $\psi_k(t)$ are the "temporal coherence modes." If only a single mode is occupied then the Stokes field is completely coherent, i.e., the modulus of the complex degree of coherence is equal to unity. If more modes are excited, then a characteristic finite correlation length and correlation time exist.

The pulse-energy operator may be written as

$$\hat{W}=\sum_n\sum_k\beta_n\hat{b}_n^{(n)\dagger}\hat{b}_k^{(n)}\ . \tag{11}$$

By substituting this into Eq. (8), the probability density function of the pulse energy may be evaluated. The parameters β_n and λ_k are found by diagonalizing the field correlation function

$$\langle\hat{E}_S^{(-)}(\mathbf{r},t)\hat{E}_S^{(+)}(\mathbf{r}',t')\rangle\cong C_\rho(\rho,\rho')C_t(t,t')\ . \tag{12}$$

The β_n, which are the relative excitation strengths of the respective spatial coherence modes $\phi_n(\rho)$, are the eigenvalues of the homogeneous integral equation which has as its kernel the correlation function $C_\rho(\rho,\rho')$. The λ_k, which give the number of photons in the respective temporal coherence mode $\psi_k(t)$, are the eigenvalues of the homogeneous integral equation whose kernel is the temporal correlation function $C_t(t,t')$. The mode functions $\phi_n(\rho)$ and $\psi_k(t)$ are the eigenfunctions of the respective integral equation. The factorization of the field correlation function into its spatial and temporal parts, as in Eq. (12), is valid only in the limit of high gain, when most of the initiating Stokes photons can be assumed to have originated in the first gain length of the medium.

The problem of determining $P(W)$ can be reduced to the problem of diagonalizing the field correlation function in its factorized form. Since $P(W)$ is composed of a convolution of the probability distributions of each of the separate modes, its shape will depend strongly on the relative excitations of the modes. Each mode has a negative exponential probability distribution, corresponding to a Bose-Einstein distribution with large mean photon number. Thus, if only a single mode is significantly excited, $P(W)$ will be approximately a negative exponential. As more and more modes are excited, i.e., the scattered radiation becomes less coherent, the central limit theorem predicts that $P(W)$ will tend toward a Gaussian. The number of modes that are significantly excited will increase as the Fresnel number F or the temporal coherence parameter $\Gamma\tau_L/gL$ increases.

III. EXPERIMENTS

A. Apparatus

A single experimental system was used to measure the Stokes pulse-energy distribution $P(W)$ over a range of conditions. A 10-nsec pump laser pulse was used and the gas pressure was varied in order to study situations where collisional dephasing was or was not important. Also, the

laser focusing was varied to change the Fresnel number. All experiments described here were performed under conditions where the gain remained unsaturated. The photon conversion efficiency was always less than 10^{-7}.

The apparatus was arranged as shown in Fig. 2. A frequency-doubled Nd:YAG laser with wavelength 532 nm was used to induce Stokes generation at 683 nm in high-pressure hydrogen gas. Scattering was from the $Q(1)$ vibrational line of molecular hydrogen, which was chosen because of its high gain and negligible dispersion, as well as being a well-characterized Raman-active medium.[16,18] Both Stokes and pump-laser pulse energies from repeated laser shots were measured and used to calculate $P(W)$.

This system was the same as that used in Ref. 2. The laser was a Nd:YAG system, consisting of a passively Q-switched, single-longitudinal-mode, stable-resonator oscillator and three stages of amplification. This produced a 10-nsec pulse, roughly Gaussian shaped in both temporal and spatial profile, which was frequency doubled in a potassium dihydrogen phosphate (KDP) crystal, to give an energy at 532 nm of about 5 mJ with a stability of $\pm 5\%$. The frequency-doubled laser beam, which was linearly polarized, was passed through a spatial filter consisting of two 2-m-focal-length lenses and a 1-mm-diam. aperture.

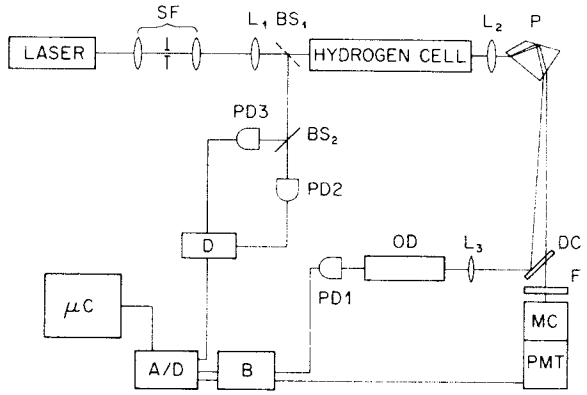

FIG. 2. Apparatus for determining the Stokes pulse-energy distribution in stimulated Raman scattering. A frequency-doubled Nd:YAG laser beam passes through a spatial filter (SF) and is collimated by a lens (L_1) to a beam of known Fresnel number. It then passes through high-pressure hydrogen and all the exiting radiation is collected by a second lens (L_2). A Pellin-Broca prism (P) serves as a dispersing element to separate the laser and Stokes frequencies, as does a dichroic mirror (DC). The Stokes light passes through colored glass filters (F) and a monochromator (MC) before being detected by a photomultiplier (PMT). The laser light passes through a 350-ns optical delay line (L_3 and OD) and is detected by a photodiode (PD1). Both detectors send electrical signals to a boxcar gated integrator (B), the outputs of which are digitized (A/D) and stored in a microcomputer (μC). In order to monitor the laser stability, a discriminator was used to suppress data acquisition on double-mode laser pulses. This consisted of two beam splitters (BS_1 and BS_2), which directed part of the laser beam onto two photodiodes (PD2 and PD3). The signals from these detectors were processed in the discriminator electronics (D), the output of which controlled the boxcar and A/D converters.

This yielded a beam that was about 1.5 times diffraction limited. The beam was focused using a single lens of long focal length (0.5–2 m) and passed through a 1-m-long stainless-steel cell with quartz windows, containing hydrogen at a known pressure, between 10 and 50 atm. The confocal parameter of the laser beam was always longer than the cell length, so that throughout the cell the beam remained approximately collimated. The cross-sectional profile of the beam was measured at the front, middle, and rear of the cell by directing the beam parallel to the cell using a mirror on a kinematic mount and allowing the light to fall on a Reticon 1024-element photodiode array. The array was read out by a transient digitizer and displayed on an oscilloscope. This allows us to measure the half-width at half maximum (a) of the intensity profile at each of the positions. The radius a at the ends of the cell was between 3% and 35% greater than at the center of the cell. This leads to an uncertainty in specifying the Fresnel number. The experimental Fresnel numbers given below are obtained by averaging the three Fresnel numbers $\pi a_i^2/\lambda_S L$, where the a_i are the measured radii at the three positions. The given range is obtained from the maximum and minimum a_i.

The average Fresnel number was varied between $F=0.3$ and 4.2. The beam passed through the cell at a slight angle in order to prevent optical feedback from the windows. On exiting the cell the laser beam and the generated Stokes light were separated using a Pellin-Broca prism, a dichroic mirror, and colored glass filters. The Stokes light was then sent to a monochromator and was incident on a photomultiplier tube (EMI 9658). The monochromator was scanned to verify that we were detecting only Stokes light at 683 nm. The laser light was sent to a fast photodiode (EG&G FND-100), used in the photoconductive mode. The current pulses from both detectors were electronically integrated with two EG&G PAR 164 boxcar integrators operating in single-shot mode. After each laser shot the outputs of the boxcars were digitized and stored in a Commodore PET 8032 microcomputer, and the boxcars were cleared.

A crucial element for the success of the experiment is that the laser pulse be highly reproducible, in both temporal shape and energy, for a given set of laser shots from which a Stokes energy probability distribution is obtained. This is because small variations of Raman gain will result in large variations of the number of Stokes photons, thus masking the quantum fluctuations of interest here. Two instabilities of the laser had to be monitored: (1) about 35% of the laser pulses were not single mode, but had two longitudinal modes lasing, which produced a 500-MHz modulation of the intensity during the pulse, and (2) the total laser pulse energy varied by $\pm 5\%$ from shot to shot. The laser pulse energy instability was easily monitored. Since the laser pulse energy was being measured to $\pm\frac{1}{2}\%$ of its mean energy, the pulses were sorted into nine separate groups, each corresponding to a different mean laser energy and each having resolution of $\frac{1}{2}\%$. For each group a Stokes pulse-energy histogram was obtained. In order to automatically reject laser shots that were double mode, the intensity modulation was detected by passing the signal from a fast photodiode (PD3) through a 100-

MHz bandpass filter centered at 500 MHz. The resulting signal was rectified and combined with the trigger signal (PD2) so that if a double-mode shot occurred, the boxcar did not receive a trigger pulse from the discriminator, and the computer did not record data on that shot.

In order to calibrate the laser energy and to determine absolutely the peak Raman gain coefficient g, the total laser pulse energy was measured using a pyroelectric detector. This was used to calibrate a silicon photodiode used in the photovoltaic mode onto which the laser beam, attenuated by known neutral-density filters, was directed. A pinhole of known diameter (either 100 or 200 μm) was then placed in the center of the beam and the fraction of the total beam energy falling within this diameter was measured. This method determined the absolute energy flux (J/cm^2) at the center of the beam, which was used to calculate the gain coefficient.

B. Results

The data were collected in the form of histograms, each corresponding to a small range of laser pulse energies. Each histogram consisted of about 250 bins. The number of Stokes pulses with energy falling in the range $W_i+\Delta W$ is denoted by N_i. The total number of pulses in each histogram, N_T, was between 5000 and 15000. The Stokes pulse-energy probability density function $P(W)$ was estimated from the histograms using the kth-nearest-neighbors method.[19] This method maintains a constant fractional statistical precision of the density estimate at the point W_i by varying the sampling window size $2h_i$ so as to keep the number of data points k_i within the window nearly equal to some chosen constant k. Thus

$$k_i=\sum_{i-h_i}^{i+h_i} N_j \cong k \ . \tag{13}$$

The density estimate for the ith bin is then given by

$$P(W_i)=\frac{1}{N_T}\frac{k_i}{2h_i} \ . \tag{14}$$

The fractional error in this estimate is $(k_i)^{-1/2}\cong k^{-1/2}$. The ratio N_T/k was taken as 50. A biasing effect occurs for points W_i near the boundaries of the range of W (large W and small W). We omit from our plots the values of $P(W)$ in these regions.

The parameters that characterize the regime of the scattering and thus the shape of the probability distribution $P(W)$ are the Fresnel number of the interaction region (F) and the temporal coherence parameter ($\Gamma\tau_L/gL$). The rate of dephasing of the molecular dipoles due to collisions (Γ) is determined by the hydrogen pressure (P). In all of our experiments the line broadening due to collisions predominated over that due to the Doppler effect. Thus $\Gamma\cong\Gamma_0 P$ where $\Gamma_0=1.65\times10^8$ rad s^{-1}/atm.[18] The pump pulse length τ_L was determined by the laser system and had the value $\tau_L\cong10$ nsec. The gain coefficient g was obtained from the measured peak laser intensity I_L using $g=g_0 I_L$, where $g_0=2.5\times10^{-9}$ cm/W was taken from Ref. 18. The length of the interaction region L was equal to 1 m in all cases. All experiments were done under conditions of unsaturated gain.

1. *Effect of dephasing collisions*

Figure 3 shows typical results from the study to determine the effects of dephasing collisions on the probability density function. The parameters for these experiments were as follows. The laser was collimated to a beam of approximately 400 μm full width at half maximum at the center of the cell, leading to an average Fresnel number of about $F=0.27(\pm0.09)$. This means that a single spatial mode is predominantly excited and the Stokes light should be spatially coherent. The pressure of the hydrogen gas was altered for each experiment in Fig. 3, from 155 psi for curve (i), to 400 psi for curve (ii), and 700 psi for curve (iii), all at room temperature. The laser power was then adjusted so that $10^{6\pm1}$ Stokes photons were generated. The peak laser intensity was typically between 35 and 55 MW/cm^2. This leads to a steady-state gain coefficient (gL) between 9 and 17.

The probability distributions in Fig. 3 rise sharply at small Stokes energies to a peak value at the most probable energy $W_{\rm MP}$, which is less than the mean energy $\langle W\rangle$. For energies between $\langle W\rangle$ and $2.5\langle W\rangle$ the probability density decreases as a negative exponential. The ratio of the most probable energy to the mean energy increases as the temporal coherence parameter $\Gamma\tau_L/gL$ increases, i.e., as the number of temporal modes that are significantly excited increases. For the most transient case, curve (i) of Fig. 3 where $\Gamma\tau_L/gL\cong1.6$, the peak of the distribution is at $W_{\rm MP}\cong0.2\langle W\rangle$, and only two or three temporal modes are significantly excited. In curve (ii) of Fig. 3, where $\Gamma\tau_L/gL\cong5$, between five and ten temporal moves are excited, and the peak of the distribution has moved to $W_{\rm MP}\cong0.5\langle W\rangle$. Finally, in curve (iii) of Fig. 3, our most steady-state case is reached. Here $\Gamma\tau_L/gL\cong11$ and the most probable energy is $W_{\rm MP}\cong0.7\langle W\rangle$. Thus we conclude that the peak of the distribution moves towards the mean as the amount of collisional dephasing increases. Also, the fractional standard deviation of the distribution decreases, and the shape tends toward a Gaussian under the same conditions. This is an example of the central limit theorem; the probability distribution is made up of adding together several independent fields, as represented by the coherence modes, leading to a Gaussian shape.

2. *Effect of transverse extent*

Figure 4 shows the results of the experiments to determine the effect of a finite transverse spatial extent of the interaction region on the probability distribution. Here the temporal coherence parameter $\Gamma\tau_L/gL$ was kept constant by monitoring the pressure of the hydrogen throughout all experiments and keeping the ratio of laser pulse energy to beam cross-sectional area constant. The focusing of the laser was then changed to yield three different values of the Fresnel number in the interaction region. Curve (i) of Fig. 4 shows that, at low Fresnel number, $F=0.27$ (±0.03), the distribution is approximately a negative exponential, with a short, sharp rise from zero at low Stokes pulses energies to the peak of the distribution at an energy $W_{\rm MP}\cong0.2\langle W\rangle$. As the Fresnel number of the interaction region is increased to $F=1.2(\pm0.1)$ the peak of the distribution moves towards the mean, i.e.,

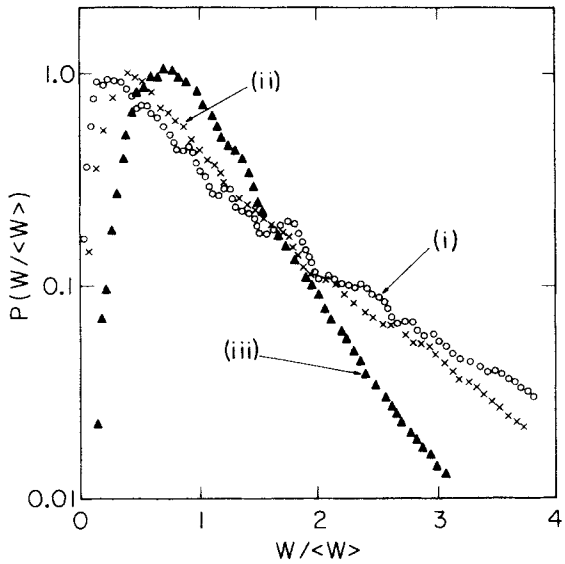

FIG. 3. Experimental Stokes pulse-energy distributions, showing the effects of collisional dephasing. Experimentally measured parameters were (i) $\Gamma\tau_L = 19$ and $gL = 15$, (ii) $\Gamma\tau_L = 49$ and $gL = 17$, (iii) $\Gamma\tau_L = 85$ and $gL = 9.4$. In all cases the photon conversion efficiency was less than 10^{-7}, and there were more than 10^6 Stokes photons per pulse. Fresnel number for all experiments was $F = 0.27$.

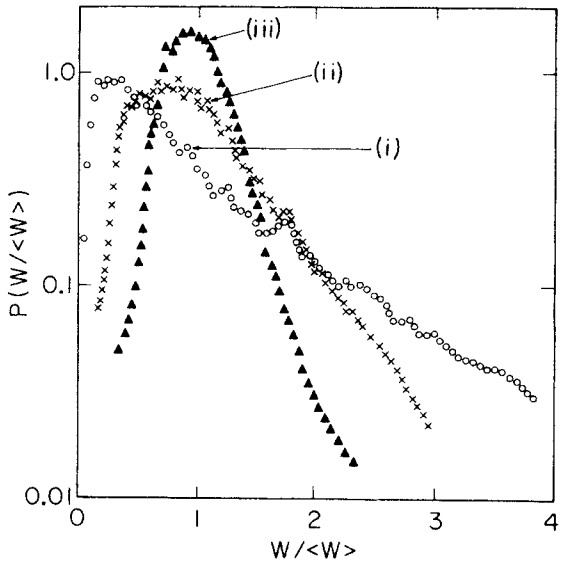

FIG. 4. Experimental Stokes pulse-energy distributions, showing the effects of the finite transverse dimension of the interaction region. Experimentally measured parameters were (i) $F = 0.27$, $\Gamma\tau_L = 19$, and $gL = 15$; (ii) $F = 1.2$, $\Gamma\tau_L = 13$, and $gL = 13$; (iii) $F = 3.8$, $\Gamma\tau_L = 12$, and $gL = 15$. In all cases the photon conversion efficiency was less than 10^{-7}, and there were more than 10^6 Stokes photons per pulse.

$W_{MP} \cong 0.7\langle W \rangle$, and its fractional standard deviation becomes smaller. When the Fresnel number is large compared to unity, i.e., $F = 3.8(+0.7, -0.5)$, the most probable energy is almost equal to the mean, $W_{MP} \cong 0.9\langle W \rangle$, and the distribution is much narrower. Notice also that it is no longer exponential in form, but closer to a Gaussian. This again can be explained as an example of the central limit theorem. The total probability density function is that of a sum of independent random fields, in this case the spatial coherence modes, and as the number of fields that are significantly excited increases, the distribution tends toward a Gaussian, even though the distributions of the individual modes are exponential. The number of spatial coherence modes which are significantly excited scales approximately as the square of the Fresnel number.

IV. COMPARISONS OF THEORY AND EXPERIMENT

The experiments described in the previous section have been modeled using the theory outlined in Sec. II. The experimentally determined values of the Fresnel number (F), the gain coefficient (gL), and the product of collision rate with laser pulse length ($\Gamma\tau_L$) were used to generate the kernel $C_\rho(\rho,\rho')C_t(t,t')$ given in Eq. (12). This was then diagonalized by numerical methods and the resulting eigenvalues were used to construct the probability density function of Stokes pulse energies, $P(W/\langle W \rangle)$, via Eq. (8). (See Ref. 17 for details.)

Using this theory with no free parameters it was not possible to obtain a good fit of theory to all of the experiments. The theory predicted that the Stokes light would be "more incoherent," i.e., more coherence modes would be significantly excited, than the experiments actually showed. This led to a most probable energy W_{MP} that was typically 15–30% higher than that observed. However, by using the gain coefficient (gL) as a free parameter, yet still taking the experimental values of F and $\Gamma\tau_L$, we were able to get excellent fits of the theoretical distributions to those of the experiments.

The resulting theoretical probability distributions are shown in Figs. 5 and 6. The dephasing study in Fig. 3 is to be compared to the theoretical plots of Fig. 5, for which the parameters used were $F = 0.273$ for all plots, and temporal coherence parameters ($\Gamma\tau_L/gL$) of 0.75 in curve (i), 1.7 in curve (ii), and 5.4 in curve (iii). These temporal coherence parameters are all a factor of 1.7 less than the experimentally determined values. The theoretical distributions fit well in terms of the position of the most probable Stokes energy and standard deviations. There is some deviation at Stokes energies greater than 2.5 times the mean. We believe this is due to the small number of points in the original experimental histograms (about 7000 shots per histogram), which leads to a biasing of the estimate of $P(W/\langle W \rangle)$. In Fig. 6 are the theoretical plots corresponding to the experimental Fresnel number study of Fig. 4. Again the experimentally determined values of F and $\Gamma\tau_L$ are used, and the gain coefficients are increased by a factor of 1.7 over the experimental values. In Fig. 6 the temporal coherence parameter was 0.75 for curve (i), 0.61 for curve (ii), and 0.50 for curve (iii). Curve (iii) in Fig. 6 was calculated using $F = 3.5$, a value which falls within the experimental error range for the measured Fresnel number, because the numerical algorithm was unstable for higher values. Using $F = 3.8$

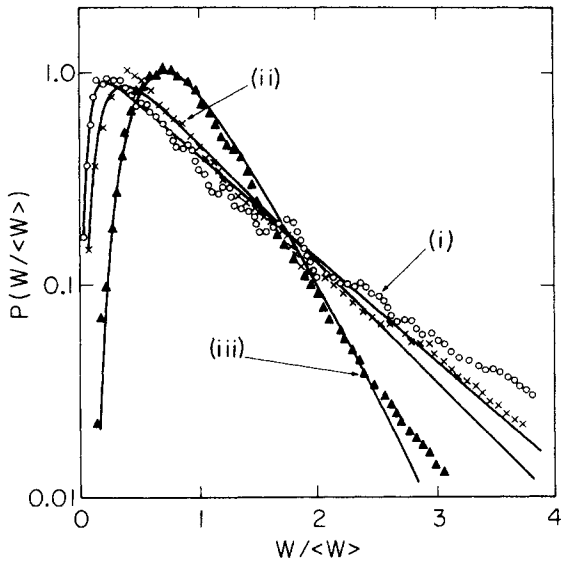

FIG. 5. Comparison of dephasing experiments to theory. Solid lines are best-fit theoretical curves; the experimental points are the same as those in Fig. 3. Parameters for the theoretical plots are (i) $F=0.273$, $\Gamma\tau_L=18.9$, and $gL=25.1$; (ii) $F=0.273$, $\Gamma\tau_L=48.7$, and $gL=28.8$; (iii) $F=0.273$, $\Gamma\tau_L=85.2$, and $gL=15.8$.

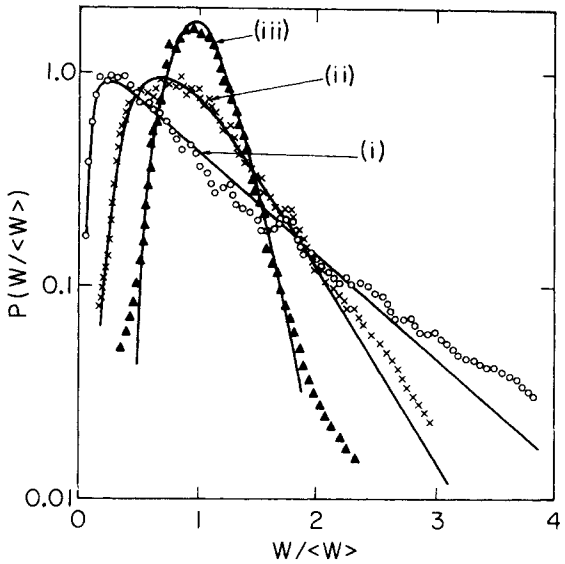

FIG. 6. Comparison of Fresnel number experiments to theory. Solid lines are best-fit theoretical curves; the experimental points are the same as those in Fig. 4. Parameters for the theoretical plots are (i) $F=0.273$, $\Gamma\tau_L=18.9$, and $gL=25.1$; (ii) $F=1.23$, $\Gamma\tau_L=13.4$, and $gL=22.1$; (iii) $F=3.5$, $\Gamma\tau_L=12.3$, and $gL=24.6$.

would result in a standard deviation of $P(W)$ that is 7% smaller than that of the curve plotted, leading to a curve that would fall within the accuracy of the experiment. The theoretical plots again fit the experimentally measured distributions. The peaks of all three $P(W/\langle W\rangle)$ are located the same as their experimental counterparts, and the only deviations occur at high Stokes energies, for the same reason as before.

It should be noted that using the adjusted value of g gives a theoretically predicted value for the mean Stokes energy $\langle W\rangle$ that is much higher than observed. The observed value is $10^{6\pm1}$ while the predicted value is $10^{8\pm1}$. This means that the need to increase g does not arise simply from an inaccuracy in our laser intensity measurement. Also, the various published values of the gain coefficient for hydrogen[16,18] differ by about 25%. Whilst we have used the most recent result[18] in our calculations, this issue is not completely settled. Our own measurement of the gain coefficient, which is accurate to within $\pm50\%$, is consistent with the published values.

There are several features of the experiment that are not accurately modeled by the theory. First, it is only possible to obtain an analytic solution to the Maxwell-Bloch equations [Eqs. (1) and (2)] under the condition that the interaction region is a uniformly pumped cylinder of well-defined radius and, consequently, Fresnel number. The experiments are performed using a laser with an approximately Gaussian spatial profile. The pumped region is neither cylindrical as assumed in the theory, nor of well-defined radius. This means both that the Fresnel number of the interaction region was not well defined, and that the gain was not uniform throughout the region. Averaging over the Gaussian profile would lead to a lower overall gain than that used in the theory. Second, the experiment at low pressure is in the regime where Doppler broadening and motional narrowing are important.[16] However, the theory used accounts only for homogeneous collisional line broadening. These inhomogeneous effects produce the same or a slightly larger linewidth than purely homogeneous broadening, but they also give rise to a non-Lorentzian line shape, which further complicates the estimate of the gain coefficient. Third, the temporal shape of the laser is assumed to be Gaussian, when, in fact, it had the shape of a normal Q-switched pulse, with a longer trailing than leading edge. This leads to an increased gain in the trailing edge of the pulse over a Gaussian pulse of the same width and area. This extra gain causes some narrowing of the spontaneous Stokes linewidth and thus a more coherent Stokes field. This effect is not thought to be a dominant one. The overall consequence of these points would seem to be that the gain is in fact lower than the value calculated from our experimental parameters, and thus they cannot explain the need to increase the value of gL to obtain a good fit of theory to experiment.

There are also several subtle questions about the condition for which the theory discussed in Sec. II is valid. The theory neglects the weak reflections of the Stokes light from the transverse boundaries of the laser-pumped region. This can lead to waveguiding effects for small Fresnel numbers ($F\ll1$). The approximate factorization of the kernel $\langle\hat{E}_S^{(-)}(\mathbf{r},t)\hat{E}_S^{(+)}(\mathbf{r}',t')\rangle$ into spatial and temporal parts as in Eq. (12) ignores the coupling between spatial and temporal coherence that occurs in propagation. These effects may be important in determining the form of $P(W)$. Another theoretical question concerns the

way in which collisional dephasing was modeled in Eq. (2). It may be argued that the dephasing, which includes contributions from elastic and inelastic collisions, cannot be well modeled by a damping constant and a delta-correlated, Gaussian, additive random noise term. In fact, it can be shown that for systems with many molecules, in the absence of saturation, it is an accurate description. Thus we do not believe this is the source of the discrepancy.

The most important effects, it seems, are those that modify the gain. We find that all of the experiments may be modeled well by increasing the gain coefficient (gL) a factor of 1.7 over its experimental value, whereas they cannot be modeled by a single uniform change in either of the other parameters (F or $\Gamma\tau_L$).

V. CONCLUSIONS

It has been experimentally shown that the Stokes pulses generated when an intense laser pulse scatters in a dispersionless medium have widely varying energies. This can be interpreted in terms of the quantum noise in the molecular dipoles which initiates the spontaneous scattering. The shape of the pulse-energy probability density function $P(W)$ which describes these fluctuations is determined by the amount of spatial and temporal incoherence in the scattering and amplification processes. The position of the peak of the distribution is found to be a sensitive probe of these incoherences.

As either the Fresnel number F or temporal coherence parameter $\Gamma\tau_L/gL$ increases, the distribution is found to become narrower and its peak moves toward the mean energy. That is, the most coherent source exhibits the largest fluctuations and the least coherent source the smallest fluctuations. This is in agreement with expectations based both on simple ideas of coherence and on a detailed three-dimensional theory, reported in Ref. 17.

Even using the detailed theory in Ref. 17, however, only qualitative agreement can be obtained. The behavior of the probability distributions of Stokes pulse energies follows the same trends as the theory, that is, the value of the most probable energy as a fraction of the mean increases, and the shape of the distribution changes from negative exponential toward a Gaussian, as the Stokes light becomes less coherent. In understanding this behavior it is useful to use the concept of coherence modes. In the purely transient regime, ($\Gamma\tau_L < gl$) only a single temporal coherence mode is excited and the shape of $P(W)$ is determined mainly by the shape and size of the interaction region. The other extreme occurs when the Fresnel number of the interaction region is small ($F < 1$), and only a single spatial coherence mode is excited. Then the shape of $P(W)$ is determined mainly by the degree of temporal coherence.

Good quantitative agreement between experiment and theory can be found only when the gain coefficient is taken as a free parameter. The gain required by the theory in order to fit the experimental data is about 70% greater than the experimental determined value. This is the same for all data sets, and is not due to any ambiguity in our measurements of the laser intensity or in the published values of the gain coefficient. This implies that there is some error in the theoretical description of the experiments. The theory is valid for a uniformly pumped cylinder of well-defined radius, whereas in practice the interaction region is not cylindrical, nor is the gain uniformly distributed throughout.

It should be pointed out that the one-dimensional theory,[1,3] which assumes spatially coherent light, is entirely inadequate for fitting the present statistical data, even for small Fresnel numbers. Using the one-dimensional theory the predicted coherence of the Stokes light, as measured by the peak of the distribution $P(W)$, is higher, for a given temporal coherence parameter, than that of the three-dimensional theory, even at Fresnel numbers as small as those in our experiments. In contrast, experimental measurements of the delay time statistics in two-level superfluorescence have been modeled with some success by one-dimensional theories, for small Fresnel numbers, although there is a need for more accurate experimental data to further test this point.[7,8]

The stimulated Stokes generation process is, for all practical purposes, a nonstationary process (i.e., the field correlation function depends on both of its time arguments and not just their difference) since SRS may only be seen using a pulsed driving laser. The application of orthogonal mode expansions to such processes is not fully understood, but in special cases gives exactly the same results as other methods,[1] and has the advantage of being applicable under a wider range of conditions. The present experiment gives some indication that the method is a sound one.

The energy fluctuations of the Stokes pulses have also been studied in the saturated regime, when the pump laser is significantly depleted. It was found that the fluctuations of the energy decreased as the process became saturated. Good agreement was found between experiment[20] and theory[21] in this case.

In summary, the experiments show that the qualitative behavior of SRS pulse fluctuations is well understood. The theoretical treatment of the problem,[17] while already quite highly developed, needs to be improved to account for the transverse Gaussian laser profile, rather than using an idealized cylindrically shaped pumped region.

ACKNOWLEDGMENTS

We wish to thank Jan Mostowski, Kazik Rzążewski, and Bożena Sobolewska for ongoing theoretical collaboration and John Carlsten for useful discussions concerning these experiments. This work was supported by the U.S. Joint Services Optics Program.

[1]M. G. Raymer, J. Mostowski, and K. Rzażewski, Opt. Lett. **7**, 71 (1982).

[2]I. A. Walmsley and M. G. Raymer, Phys. Rev. Lett. **50**, 962 (1983).

[3]M. G. Raymer and I. A. Walmsley, in *Proceedings of the Fifth Rochester Conference on Coherence and Quantum Optics, June 1983,* edited by L. Mandel and E. Wolf (Plenum, New York, 1984), p. 63.

[4]N. Fabricius, K. Natterman, and D. Von der Linde, Phys. Rev. Lett. **52**, 113 (1984).

[5]D. Meltzer and L. Mandel, Phys. Rev. A **3**, 1763 (1971); S. M. Curry, R. Cubeddu, and T. W. Hänsch, Appl. Phys. **1**, 153 (1973).

[6]S. P. Kravis and L. Allen, Opt. Commun. **23**, 289 (1977); S. P. Adams and N. Abraham, in Ref. 3, p. 233.

[7]F. Haake, H. King, G. Schröder, J. Haus, and R. Glauber, Phys. Rev. A. **20**, 2047 (1979); D. Polder, M. F. H. Schuurmans, and Q. H. F. Vrehen, *ibid.* **19**, 1192 (1979).

[8]Q. H. F. Vrehen and J. J. der Weduwe, Phys. Rev. Lett. **45**, 558 (1980), Phys. Rev. A **24**, 2857 (1981); P. D. Drummond and J. H. Eberly, *ibid.* **25**, 3446 (1982); J. Mostowski and B. Sobowlewska, *ibid.* **28**, 2573 (1983); **30**, 1392 (1984).

[9]P. Lett, W. Christian, S. Singh, and L. Mandel, Phys. Rev. Lett. **40**, 1982 (1981).

[10]J. Mostowski and M. G. Raymer, Opt. Commun. **36**, 237 (1981); M. Raymer and J. Mostowski, Phys. Rev. A **29**, 1980 (1981).

[11]T. von Foerster and R. J. Glauber, Phys. Rev. A **3**, 1984 (1971).

[12]R. L. Carman, F. Shimizu, C. S. Wang, and N. Bloembergen, Phys. Rev. A **2**, 60 (1970).

[13]J. Mostowski and B. Sobolewska, Phys. Rev. A **30**, 610 (1984).

[14]K. Rzążewski, M. Lewenstein, and M. G. Raymer, Opt. Commun. **43**, 451 (1982).

[15]M. Lewenstein, Z. Phys. B **56**, 69 (1985); M. Trippenbach and K. Rzążewski, Phys. Rev. A **31**, 1932 (1985).

[16]E. E. Hagenlocker, R. W. Minck, and W. G. Rado, Phys. Rev. **154**, 226 (1967).

[17]M. G. Raymer, I. A. Walmsley, J. Mostowski, and B. Sobolewska, Phys. Rev. A **32**, 332 (1985).

[18]W. Bischel and M. J. Dyer, J. Opt. Soc. Am. **73**, 1867 (1983); W. Bischel (private communication). The values of Γ_0 and g_0 reported here are within 30% of those reported in Ref. 16.

[19]See, for example, J. Friedman, Stanford Linear Accelerator Center Report No. 176, 1974 (unpublished).

[20]I. A. Walmsley, M. G. Raymer, T. Sizer II, I. N. Duling III, and J. D. Kafka, Opt. Commun. **53**, 137 (1985).

[21]M. Lewenstein, Z. Phys. B **56**, 69 (1985).